CHEMISTRY OF MATERIALS

ARTICLE

pubs.acs.org/cm

Photochemical Grafting and Patterning of Metallic Surfaces by Organic Layers Derived from Acetonitrile

Avni Berisha,[†,‡] Catherine Combellas,[†] Géraldine Hallais,[§,∥] Frédéric Kanoufi,[†] Jean Pinson,[*,†] and Fetah I. Podvorica[†]

[†]Physico-Chimie des Electrolytes, des Colloïdes et Sciences Analytiques, ESPCI, CNRS UMR 7195, 10 rue Vauquelin, 75231 Paris Cedex 05, France

[‡]Chemistry Department of Natural Sciences Faculty, University of Prishtina, rr. "Nëna Tereze" nr. 5, 10000 Prishtina, Kosovo

[§]Alchimer, 15 rue du Buisson aux Fraises, 91300, Massy

Supporting Information

ABSTRACT: Metallic substrates are modified by a polymeric layer obtained under photochemical irradiation of acetonitrile. The reaction involves a photogenerated radical and leads to the covalent bonding of the organic layer to the metal. Different characterization techniques allow to unravel the structure of the layer: *Substrate*-CH_2-CH-(NH_2)[-CH_2-CH-(NH_2)-]$_n$-[CH_2-C(=O)]$_m$. A mechanism is discussed that accounts for the formation of the layer. The method is quite easy to implement, it only necessitates a UV lamp and a very common solvent. Photografting is well suited to pattern surfaces with polymeric layers by irradiation through a mask, and finally, the patterning of copper at the micrometer scale is described as a proof of concept.

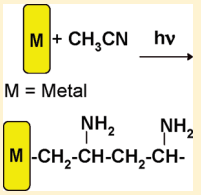

KEYWORDS: photochemistry, surface modification, patterning, acetonitrile

INTRODUCTION

Electrografting is a well recognized technique for the covalent modification of surfaces, for example, by reduction of vinylics or diazonium salts.[1,2] These methods permit to obtain strongly bonded organic layers on carbon, metals, semiconductors, and dielectric substrates. Such coatings range from monolayers to micrometric thick polymer layers and can include a very large number of organic functions.

Some examples of localized electrografting of surfaces have been published. A first series of experiments use atomic force microscopy (AFM) for patterning surfaces. For example, the localized electrografting of diazonium salts has been achieved by electrografting a uniform film, removing lines of the film with an AFM tip, and electrografting a second diazonium in the lines.[3] In this way, patterns down to 0.33 μm width of methyl and nitro groups were obtained on a flat carbon surface. AFM also permitted the targeted delivery of a single molecule.[4] For that, gold coated AFM tips were modified by electrografting a vinylic polymeric chain that reacts with the surface when the tip is brought into contact. When the tip is retracted the weakest bond between the tip and the surface is broken (Au(tip)−C(vinylic polymer) bond) and finally the polymer chain remains bonded to the surface.

A second method used poly(dimethylsiloxane) (PDMS) molds with 22 μm channels that were applied on flat carbon surfaces. The channels were filled with a diazonium salt that was electrografted. Spontaneous grafting of metallic surfaces can also be achieved with this technique,[5] as well as the modification of already grafted layers.[6] Instead of using a stamp, a Au or GC surface has been covered with an array of polystyrene beads (down to 0.1 μm) that mask part of the surface. Then, the aryldiazonium electrografting process is followed by subsequent removal of the polystyrene beads; the ungrafted surface areas become available for either another aryldiazonium electrografting or a metal electrodeposition.[7]

SECM (Scanning ElectroChemical Micoscopy) permits to pattern conductive and insulating surfaces. A nitro aryl derivative is reduced at the tip of a SECM to an amine and as this amine diffuses to the substrate, it is diazotized (by $NaNO_2$ added in the solution) and the diazonium salt is reduced and electrografted on the substrate maintained at −0.1 V/SCE; 40 μm wide spots were obtained.[8] Organic bands (110 μm wide) were electrografted onto a gold surface by direct reduction of a diaryliodonium ion at the surface, the SECM tip acting as a counter-electrode.[9] Since an organic layer of bromobenzyl groups attached to a gold substrate acts as an initiator for ATRP (Atom Transfer Radical Polymerization), by locally reducing the C−Br bond, no polymerization is possible where the bromine atoms have been cleaved and a ∼ 100 μm pattern was obtained in the polymeric layer.[10,11] By electrogenerating highly reducing radical anions at a SECM tip, it was possible to reduce 200 μm spots of polytetrafluoroethylene into carbon and to attach a polymer to this carbon.[12] By reducing a solution containing a diazonium and a vinylic, intricate deposited polymer patterns made of ∼0.2 μm lines were obtained by atomic force-scanning electrochemical microscopy (AFM-SECM).[13]

On semiconductors, localized doping may promote localized electrografting; this was demonstrated, for example, on p-doped Si(100) covered with its native oxide.[14−16] It is also possible to produce localized electrografting by using surfaces made of two

Received: February 24, 2011
Revised: June 20, 2011
Published: July 06, 2011

different materials. With a silicon sample partly plated with gold,[17] only the gold part of the sample is electrografted whatever silicon or gold is used for contact. In this way, thin patterns such as interdigitated gold electrodes with 0.5 μm between the two electrodes can be selectively covered with polymeric films.

Looking at these different methods for patterning polymers on surfaces, it appears that SECM and AFM are very slow methods that will be difficult to use on a larger size than a few μm; the use of PDMS stamps seems also difficult on a production scale. On the contrary, photopatterning is widely used by the microelectronic industry to produce integrated circuits with patterns down to 32 nm and the fabrication of very complicated masks is now routinely achieved by this industry. In the biological field, biomicropatterning onto polyethyleneglycol covered glass using deep UV light is an elegant method to control cell adhesion geometry on surfaces.[18] It would therefore be interesting to find out photochemical methods for patterning various substrates including metals and carbon, starting from simple chemicals.

Among the already existing photografting methods, the modification of the surface of polymers has been the most widely investigated. Some examples involve the grafting of (i) polyethylene by acrylic acid in the presence of benzophenone or formaldehyde,[19−21] (ii) benzoylated polystyrene by polyethyleneglycol chains to give a polystyrene-graft-polyethyleneglycol,[22] (iii) polydimethylsiloxane by polyvinylic acid.[23] In a different reaction, alkenes and alkynes have been grafted, under irradiation, on a variety of substrates (diamond,[24−38] glassy carbon,[39−43] pyrolyzed photoresist,[44] amorphous carbon,[45] carbon nanotubes,[46] silicon[47−56]). These alkenes or alkynes can be end functionalized to permit further modification.[37,57] Alkyl halides have also been photografted on diamond (hydrogenated or not) and metal surfaces, using X-ray beams or UV irradiation.[58−60]

Heterocyclic azides[61] and other substituted phenyl azides[62] can be photopatterned by UV through masks onto polymer surfaces (polyethylene, polyimide, polyester, etc.), giving micrometer sized patterns on polystyrene.[62] Patterning through a photoresist is also possible.[63] A photoresist deposited on Si(100) was irradiated through a mask; after lift-off, a diazonium salt was electrografted on Si to give patterns of 4-aminophenyl groups (down to 1 μm).[64]

In this paper, we present a method for photografting a very simple compound, acetonitrile (ACN) or haloacetonitriles, to give nanometer thick amino layers. When irradiation takes place through a mask, 100−200 μm wide lines are obtained.

In a recent paper, the electrochemical reduction of I- and Br-CH_2CN was reported to give an amino layer through an intermediate cyanomethyl radical ($^{\bullet}CH_2CN$).[65] The indirect electrografting of ACN has also been described by reducing 2,6-dimethylphenyl diazonium.[66] Because of the steric hindrance of the two methyl groups, the 2,6-dimethylphenyl radical obtained cannot bind to the substrate,[67] but it can abstract an hydrogen atom from the solvent (ACN). This leads to the cyanomethyl radical that reacts with the metallic (Au, Cu) or Si−H surfaces to give a bonded organic layer that can be described as *Substrate*-$[CH_2CH(NH_2)]_n$ with carbonyl groups included in the chains. A mechanism has been proposed to account for the formation of this layer.

Photografting of ACN was also observed on Carbon Nano-Tubes (CNT), and the following structure was assigned to the modified nanotubes: *CNT*-CH_2-CH_2-NH_2 on the basis of XPS and IR spectra, without any evidence concerning the thickness of the film and the mechanism for its formation.[68] As we will see below our results do not agree with this structure.

EXPERIMENTAL SECTION

Chemicals. Anhydrous acetonitrile (99.8%), 4-nitrobenzoyl chloride, 4-*tert*-butyl, and 4-nitrophenyl isocyanate were from Sigma-Aldrich and iodoacetonitrile (ICH_2CN) from Acros Organics. They were used as received. One irradiation experiment was performed with a freshly opened bottle of 99.9% Chromasolv ACN; similar IR spectra were observed on copper (Supporting Information, Figure. S1). Acetone, sulphuric acid (96%) were from Acros Organics and hydrogen peroxide (30%) from Merck Schuchardt. Milli-Q water (>18 MΩ) was used for plate rinsing and solutions preparation. ***Caution!*** *ICH_2CN should be handled with gloves.*

Plates. One 1 × 1 cm^2 gold coated wafers (Aldrich, gold coated silicon wafer, 1000 Å coating) were cleaned with "piranha" solution (1:3 v/v H_2O_2:H_2SO_4) for 10 min at room temperature, and rinsed under sonication for 10 min in Milli-Q water. Before modification, the plates were dried under a stream of nitrogen. ***Caution!*** *Piranha solutions are highly aggressive and should be handled with full protection, gloves, mask, and so forth.*

Massive (1 cm^2) iron or nickel plates were polished using 2 μm alumina slurry on DP-NAP polishing cloth with a Mecatech 234 polishing machine (Presi). For the measurements on copper, Si wafers covered with 150 nm of polished copper were used without further polishing; they were rinsed with Milli-Q water, left for 10 min into 5% aqueous solution of citric acid, rinsed again with Milli-Q water and sonicated for 10 min in acetone, and dried under a stream of nitrogen.

Photografting. Photochemical modification was achieved via wide spectrum UV irradiation mercury Pen Ray lamp UVPC-86079 (20 mA AC, 4400 μW cm^{-2} at 254 nm for a distance of ∼2 cm) with emission at 184.9 (3%, ∼ 150 μW cm^{-2}), 253.6 (100%,), 312.5−313.1,356.0−356.3, 407.7, 435.8 nm. Prior to irradiation, a thin film of neat ACN or ICH_2CN was deposited onto the metallic plates that were placed 4 cm under the UV light source. The experiments were performed in the laboratory atmosphere with some exceptions in a glovebox containing less than 1 ppm O_2. After UV irradiation for 10, 20, or 30 min, the plates and wafers were rinsed with ACN, acetone, ultrasonicated for 10 min in acetone two times, and finally ultrasonicated for 10 min in toluene. For localized photografting, the Teflon mask was held on top of the Cu wafer, and the chromed quartz mask was separated from the copper wafer by a Teflon ribbon (0.225 mm), so that a thin layer of ACN was present between the mask and the metal surface. The irradiation time was longer than without the mask (40 min) because the light intensity at the surface was lowered by the presence of the mask.

For the identification of amine groups, a copper wafer irradiated for 10 min and rinsed under sonication in acetone for another 10 min was reacted overnight in an ACN saturated solution of 4-nitrobenzoyl chloride; some corrosion of the layer was observed. In other experiments, copper wafers irradiated for 2 min in ACN and rinsed as above were derivatized in 5 mL of toluene and 300 μL of 4-*tert*-butylphenylisocyanate or 5 mL of DMF and 300 μL of 4-nitrophenylisocyanate, left overnight, and rinsed in acetone for 480 s under sonication.

Instrumentation IR. Spectra of modified plates were recorded using a purged (low CO_2, dry air) Jasco FT/IR-6100 Fourier Transform Infra Red Spectrometer equipped with MCT (mercury-cadmium-telluride) detector. For each spectrum, 1000 scans were accumulated with a spectral resolution of 4 cm^{-1}. The background recorded before each spectrum was that of a clean substrate. The profiles were recorded with an IRRAS Jasco IRT 700S microscope, using a 40 × 40 μm^2 beam size and 800 accumulations with a spectral resolution of 4 cm^{-1}.

Thicknesses. Thicknesses of the films on Au and Cu were measured with a mono wavelength ellipsometer Sentech SE400. The following

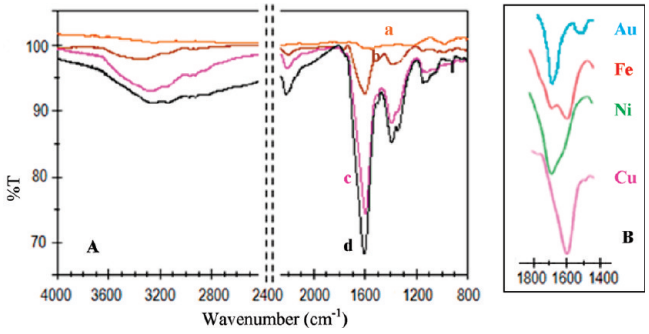

Figure 1. IRRAS spectra of (A) a copper wafer (a) left in ACN without irradiation for 30 min; (b−d) submitted to UV irradiation in ACN for (b) 10, (c) 20, and (d) 30 min and (B) the 1500−1800 cm^{-1} range for Au, Fe, Ni, and Cu, photografted for 20 min (C═O stretching and NH_2 deformation bands). Ultrasonication for 10 min in acetone after photografting.

values were taken for gold: ns = 0.153, ks = 3.567; for copper: ns = 0.101, ks = 3.513. These values were measured on clean surfaces before photografting, and the film thicknesses were determined from the same plates after modification, taking ns = 1.46, ks = 0 for the polymeric layer.

The thickness profile was recorded with an interferometric profilometer Microsurf 3D from Fogale. The real thickness reported in Figure 6, *z*, is obtained from the interferometric profile (not shown). This profile presents a height decrease in the pattern region where a layer was expected to have grown. This is explained from the loss of light reflectivity induced by the beam light transport into the dielectric grafted layer: the ungrafted copper surface is more reflecting than the copper surface covered by a thin dielectric layer. The interferometric topographic profile, Z_{topo}, is converted into local grafted film thickness, *z*, from $z = -Z_{topo}/2n$ where $n = 1.46$ is chosen for the grafted layer refractive index.

Contact angles. They were measured using the Krüss DSA30 instrument. The samples were horizontally placed on the instrument stage, and 3 μL of Milli-Q water was automatically delivered on the top of the sample. At least five measurements were made for each sample. The values of the contact angles were calculated by the tangent method using Drop Shape Analysis software.

AFM images. AFM measurements were performed using a 5100 Atomic Force Microscope (Agilent technologies- Molecular Imaging) operated in a dynamic tip deflection mode (Acoustic Alternating Current mode, AAC). All AFM experiments were done using Silicon Probes (Applied NanoStructures-FORT) in the tapping mode with 3 N m^{-1} spring constant at 69 kHz. The images were scanned in topography, amplitude, and phase mode with a resolution of 512 × 512 pixels and are representative of 1 × 1 μm^2 regions over different locations on the studied surfaces.

ToF-SIMS. Spectra were obtained with an ION-TOF IV with Au^+ primary ions at 25 keV, the analyzed zone was 150 μm^2, and the acquisition time 75 s. Blank samples were analyzed in the same run as the modified samples. The peak intensity refers to the area of the peak normalized to the total intensity of the spectrum. The images were obtained with Au_3^+ ions for 100 scans (∼ 40 min).

Scanning electron microscopy (SEM) images and energy-dispersive X-ray (EDS). Spectra were obtained using a Hitachi S-4300 microscope.

Solution Analysis. Acetonitrile was irradiated for 1 h, evaporated to about one tenth of its initial volume, and diluted (50/50) with 0.1% phosphoric acid and injected by electrospray in positive mode in a Q-Tof-2 mass spectrometer from Micromass (*m*/*z* in the 90−1600 range, scan time = 1 min, inter scan time = 0.1 s, capillary voltage = 3.0 V, cone voltage = 40 V, MCP = 2100 V, source temperature = 150 °C, desolvation temperature = 300 °C).The chemical formula was obtained from the best match of the isotopic mass using the ChemCalc software.

Table 1. IRRAS Spectra of the Different Metallic Surfaces Modified with ACN under UV Irradiation. Wavenumbers in cm^{-1}

metal	peak position cm^{-1}	peak assignment
Cu	3300	-NH_2 stretching
	∼1670 sh	C═O stretching
	1600	-NH_2 deformation
Au	3260	-NH_2 stretching
	1690	C═O stretching
Ni	3320	-NH_2 stretching
	1675	C═O stretching
	∼1600 sh	-NH_2 deformation
Fe	3400	-NH_2 stretching
	1685	C═O stretching
	1600	-NH_2 deformation

RESULTS

Since acetonitrile absorbs below 200 nm, photochemical modification of metallic surfaces was achieved by irradiating at 184.9 nm a thin film of neat ACN deposited onto the metallic plate (4 cm under the UV light source). The irradiation time varied from 10 to 30 min. After irradiation, the samples were rinsed under different conditions, as described in the Experimental Section. After the initial rinsing, IRRAS spectra did not change upon further 15 min rinsing in acetone under sonication. This indicated that the layers are bonded to the surface.

IRRAS and Ellipsomeric Measurements. Without irradiation, no significant spectrum is observed. The IR spectra of copper surfaces UV irradiated for different times are presented in Figure 1. The main features of these spectra are the presence of a weak -C≡N stretching band at 2211 cm^{-1} (2254 cm^{-1} for ACN itself) and the presence of bands corresponding to grafted amino groups at 1600 cm^{-1} (NH_2 deformation) and at 3300 cm^{-1} (−NH_2 stretching). A band at 1399 cm^{-1} (CH_2 scissoring) is also observed.[66,69] Upon increased irradiation time, the transmittance decreases, which indicates the formation of thicker films (same for Au, see Supporting Information, Figure S1). The spectra obtained with Au, Ni, and Fe are presented in Supporting Information, Figures S2−S4 along with the blank experiments without irradiation, and the main peaks are assigned in Table 1. IR bands in similar wavenumber ranges are observed for all metals, but the NH_2 deformation band cannot be distinguished on Au.

For comparison, the spectra of a copper wafer irradiated in a solution of neat ICH_2CN was recorded (Figure 2; bands at 3280, 1600, 1420 cm^{-1}); it is similar to that of a copper wafer irradiated in ACN and the transmittance also decreases with time.

The IRRAS data reported in Table 1 favor the presence of −NH_2 groups on copper, gold, nickel, and iron surfaces after UV irradiation (by comparison with neat isopropyl amine: 3358, 3282, 1608 cm^{-1}, with isopropylamine chemisorbed on Ni:[70] 3300 cm^{-1}, and with a Self-Assembled Monolayer of 11-amino-1-undecanethiol that presents a broad band in the 3100−3400 cm^{-1} region[71]). Carbonyl groups are also observed (1670−1690 cm^{-1}), by comparison with acetone (1715 cm^{-1}) and with 4-hydroxy-4-methylpentan-2-one,[72] where a hydroxyl group located in the

dx.doi.org/10.1021/cm200579b |*Chem. Mater.* 2011, 23, 3449–3459

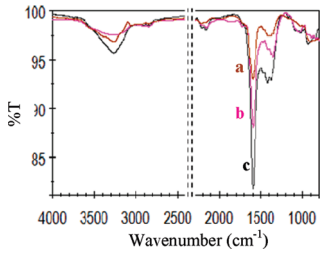

Figure 2. IRRAS spectrum of a copper wafer irradiated in neat ICH_2CN for (a) 10, (b) 20, and (c) 30 min. Ultrasonication for 10 min in acetone after photografting.

Scheme 1. Reaction of Surface Amino Groups from an Irradiated Copper Wafer with 4-Nitrobenzoyl Chloride

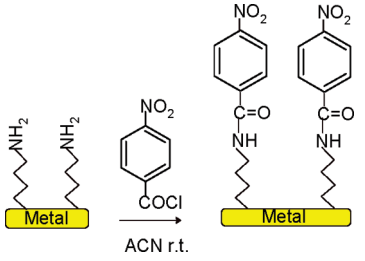

β-position (1707 cm^{-1}) is hydrogen bonded (we could not find data with a β-substituted NH_2 group). Figure 1B presents an enlargement of the 1400−1800 cm^{-1} region that shows the relative variation of the C═O stretching and -NH_2 deformation bands with the different metals.

To understand the origin of the carbonyl band, we have recorded the IRRAS spectra of gold wafers irradiated in a glovebox containing less than 1 ppm of dioxygen (Supporting Information, Figure S5) and of copper wafers prepared to minimize or increase the amount of surface oxides. On gold, in the presence of dioxygen, a C═O band can be observed at 1690 cm^{-1} (Figure 1B) and there is no significant band at ∼1600 cm^{-1}; in absence of dioxygen, the C═O band shifts to 1677 cm^{-1} because of overlapping with another band at 1616 cm^{-1}, that can be assigned to the NH_2 deformation (Supporting Information, Figure S5). Therefore, even in the absence of dioxygen, a C═O band is still present, this indicates that the oxygen of the carbonyl groups comes, at least in part, from surface oxides. This experiment also shows that in the absence of dioxygen, an NH_2 deformation band appears, that was not observed in the presence of dioxygen and therefore the formation of the C═O and NH_2 groups should be in competition. However, in these experiments, the surfaces have been sonicated before and after irradiation and it has been shown that bare Au surfaces are subject to uncontrollable, solvent dependent changes during sonication; such sonication prior to grafting may increase the reactivity of surface oxides.[73]

To ascertain the presence of amino groups, the modified copper wafers have been reacted with 4-nitrobenzoyl chloride (Scheme 1).

After reaction, the IRRAS spectrum (Figure 3) shows the disappearance of the 1600 cm^{-1} band because of NH_2 deformation and the appearance of several bands at 1692 cm^{-1} (overlapping C═O and NH amide bands), 1604 cm^{-1} (aromatic ring), and the two strong antisymetric (1532 cm^{-1}) and symmetric (1350 cm^{-1}) bands of the nitro group. The spectra of irradiated copper surfaces post modified with 4-butyl or 4-nitrophenylisocyanate are presented in Supporting Information, Figure S6; the reaction is sluggish, and the characteristic bands are small.

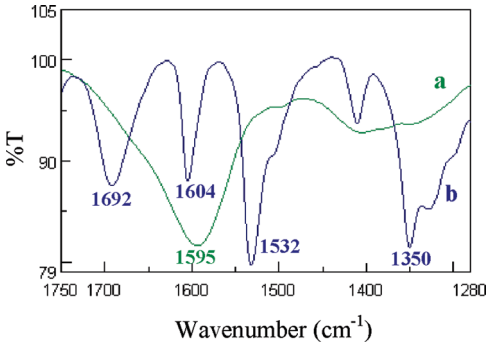

Figure 3. Copper wafer (a) photografted by UV irradiation in ACN for 10 min, and (b) immersed overnight in a saturated solution of 4-nitrobenzoyl chloride. Ultrasonication for 10 min in acetone after reaction.

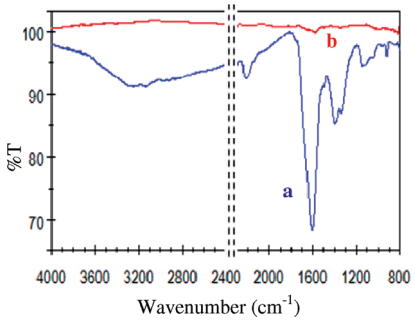

Figure 4. Copper wafer irradiated in ACN for 20 min (a) and (b) in the presence of 1% TEMPO. Ultrasonication for 10 min in acetone after irradiation.

To determine a grafting mechanism, water (1%) or acetic acid (1%) was added to ACN during irradiation of a copper wafer and no change of the IRRAS spectrum was observed, (Supporting Information, Figures S7 and S8). Conversely, when a radical trap, TEMPO (2,2,6,6-tetramethylpiperidine 1-oxyl), was added to ACN (1%, 60 mM), photografting was completely suppressed as shown in Figure 4.

The homogeneity of the layer was examined by recording IRRAS profiles at 1600 cm^{-1} along a ∼ 1 × 0.2 mm^2 line on a copper wafer (Figure 5). The profiles show that after 10−30 min irradiation, the absorbance does not present any zero value, which indicates that there is no ungrafted region at the 30 μm scale. The mean absorbance, A, increases with the irradiation time, (a) 10 min, A ≈ 0.01; (b) 20 min, A ≈ 0.02; (c) 30 min, A ≈ 0.025, indicating thicker layers as the photografting time increases, in agreement with the IR spectra (Figure 1). Some bumps are observed on these profiles.

Thickness of the Layers. The values (d) obtained by ellipsometry on copper and the relative intensity of IR absorption at 1600 cm^{-1} are represented in Figure 6 for different irradiation times in ACN. A good correlation between ellipsometric and IR measurements is observed altogether. Both vary quasi linearly with time.

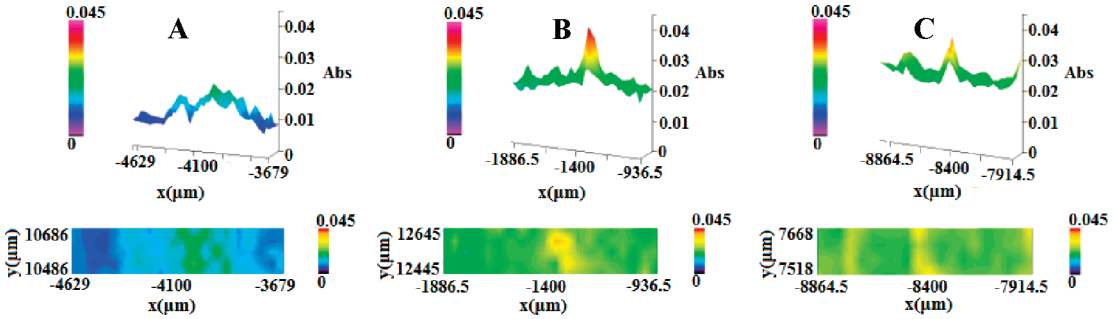

Figure 5. IRRAS surface absorbance profiles at 1600 cm^{-1} of a copper wafer photografted in ACN with irradiation time: (A) 10, (B) 20, and (C) 30 min. 40 × 40 μm beam size.

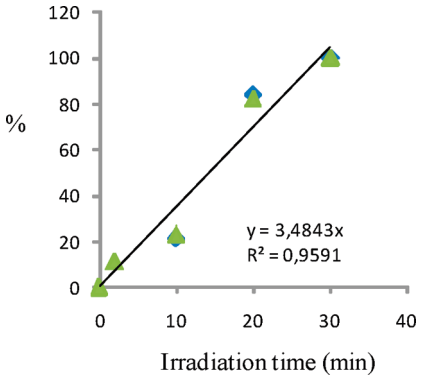

Figure 6. Relative IR intensities of the 1600 cm^{-1} band (green solid triangles) and thickness (z) (blue solid diamonds) vs irradiation time on copper wafers. A relative 100% thickness corresponds to 85 nm.

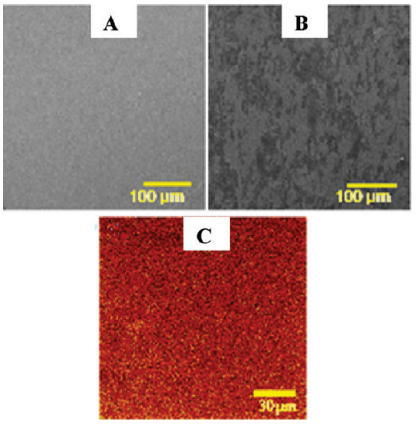

Figure 7. (A, B) **SEM** image of (A) a bare copper wafer; (B) the same wafer photografted by UV irradiation under ACN for 30 min; (C) ToF-SIMS image obtained from the sum of the positive ions (fragments containing both Cu and C), UV irradiation in ACN for 30 min.

Scanning Electron Microscopy (SEM) and Energy Dispersive Spectroscopy (EDS). Figure 7A presents the SEM images of a bare copper wafer and Figure 7B the same wafer after 30 min irradiation in ACN. The two images are clearly different, and a coating can be observed on the photografted sample (Figure 7B). To confirm that the difference in the two images of Figure 7 corresponds to the grafted organic coating, we have recorded the

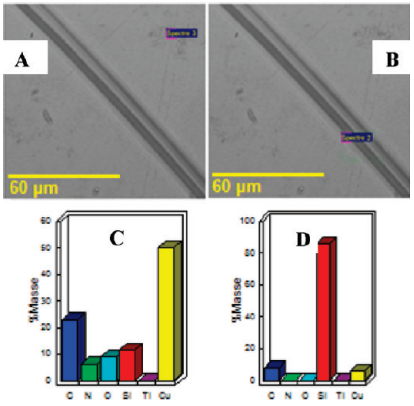

Figure 8. (A, B) EDS images of a copper wafer after 30 min irradiation in ACN. (C, D) Relative mass distribution of C, N, O, Si, Ti, and Cu atoms at the grafted surface and scratched line of the copper wafer: (C) on the modified surface along the rectangle indicated in A; (D) in the center of the scratched line along the rectangle indicated in B.

EDS spectra of the modified copper wafer at two different positions: the first one corresponds to the organic layer, the second one to the interface between the organic layer and a scratched line (Figures 8A,B).

Inside the grafted layer (Figures 8A, C), besides Cu and Si, a small amount of Ti (that probably corresponds to an intermediate layer of the wafer) is observed (~ 22% C, 8% N, and 9% O, mass %). Inside the scratch, most of the Cu has been removed (Figure 8B, D), Si appears (60−85%), C decreases to ~6%, N and O become negligible. This is in good agreement with the IRRAS spectra and confirms the presence of an organic layer containing C, N and also O.

AFM. Images have been captured on copper and gold (Figure 9). With both metals, the layer appears compact. The film thickness on copper is ~20 nm, in good agreement with the ellipsometric measurements; on gold, the layer is very thin and close to a monolayer. Supporting Information, Figures S9 and S10) present the topographic, phase, and amplitude AFM images. The topographic profiles present some dips that should correspond to small (10−100 nm diameter) holes in the layer.

ToF-SIMS. Spectra have been recorded for photografted Cu and Au surfaces. The main characteristic peaks are presented in Figure 10. Figure 10A presents negative ions assigned to NH (m/z = 15.01) and CN (m/z = 26.00), indicating the presence of nitrogen on the surface. Figure 10B presents some positive ions

dx.doi.org/10.1021/cm200579b |*Chem. Mater.* 2011, 23, 3449–3459

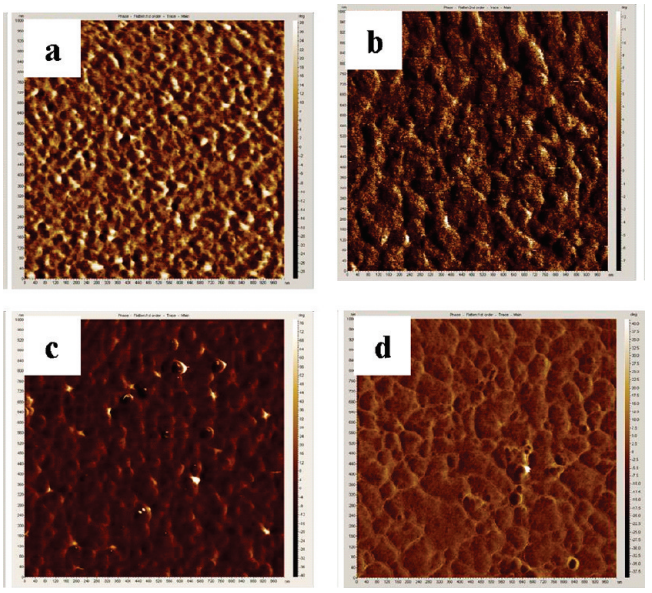

Figure 9. AFM phase images ($1 \times 1\ \mu m^2$) of copper and gold wafers (respectively a, b,) and after irradiation for 10 min in ACN (respectively c, d).

characteristic of the structure of the layer: C_4H_8NO [m/z = 86.06, CH_2-$CH(NH_2)$-CH_2-C(=O)-H], $C_4H_{10}N_2$ [m/z = 86.09, CH_2-$CH(NH_2)$-CH_2-$CH(NH_2)$-], and $C_4H_9N_2$ [m/z = 85.08, CH_2-$CH(NH_2)$-CH_2-CNH_2-] on copper; $C_6H_{15}N_2$ [(m/z = 115.12, CH_2-$CH(NH_2)$-CH_2-$CH(NH_3)$-CH_2-CH_2] on gold. Figure 10C presents positive ions that contain both an atom from the substrate (Cu, Au) and carbon from the organic layer: CuCHN [m/z = 89.94],[63] CuC_2H_3N [m/z = 103.96,[63] $CuCH_2$-NH], AuC_2N [m/z = 234.96]. Figure 7C is a 150 × 150 μm^2 ToF-SIMS image of the sum of all the positive ions containing a copper atom and a carbon fragment. As the MEB images, it indicates a homogeneous grafting. Note that, on gold, although the IRRAS NH_2 deformation band is too small to be distinguished from the neighboring C=O band, ToF-SIMS, that is more sensitive, allows observing the presence of NH_2 groups in the layer.

Analysis of the Irradiated Solution. After irradiation, a sample of acetonitrile was analyzed by electrospray ionization mass spectroscopy. The spectrum presents the base peak at m/z = 242.605 (relative intensity 100%) and smaller peaks at m/z =243.625 (32%); 409.35 (5%); 429.26 (12%); 430.28 (5%). The base peak can be assigned to the protonated oligomer ($C_{11}H_{26}N_6$, exact monoisotopic mass: 242.222), in good agreement with the proposed structure of the organic layer:

$$NC\text{-}[CH_2\text{-}CH(NH_3^+)]_4\text{-}CH_2CN$$

Open Circuit Potential (ocp) under Irradiation. To assess the possible involvement of electron transfer between the metallic substrate and the organic layer, we have measured the ocp without and under irradiation and compared these data with the ratio of amino to keto groups measured by IRRAS (Table 2, Supporting Information, Figures S11−14).

The ocp increases (becomes less cathodic) in the order Cu, Au, Ni, Fe. This order of ocp is different from that of the ratio of the IRRAS intensities of the amino deformation over the carbonyl stretching bands (Cu, Fe, Ni, Au).

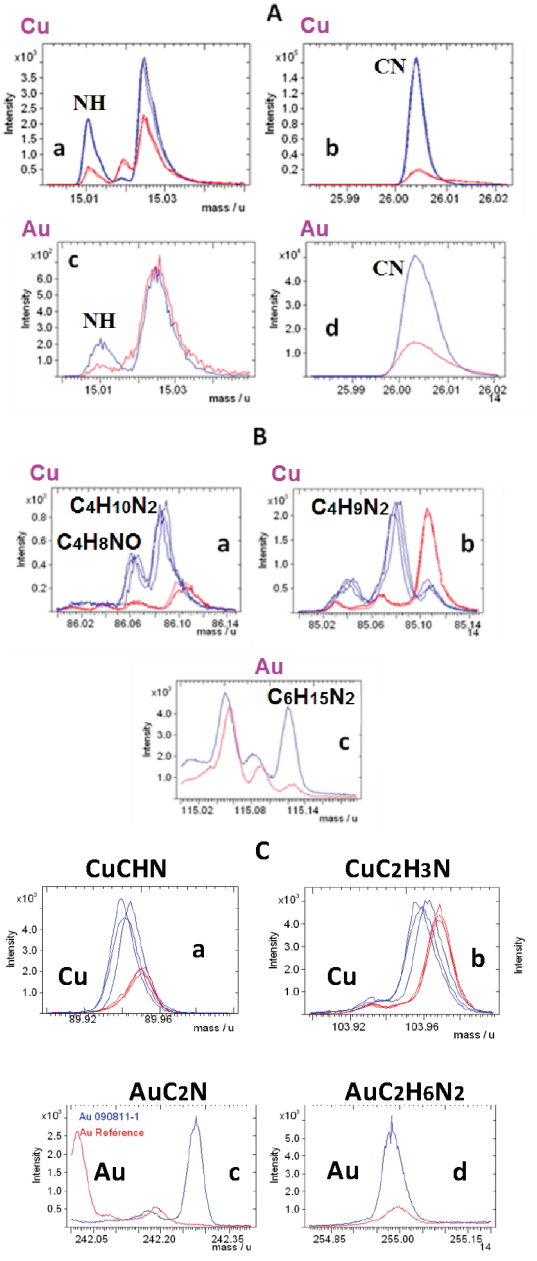

Figure 10. ToF-SIMS spectra. (A) negative ions, (B, C) positive ions; (a, b) copper wafer, (c, d) gold wafer. Blue lines: samples irradiated in ACN for 30 min; red lines: untreated samples. Some spectra are recorded three times on three different locations on the sample.

Localized Grafting. To obtain patterned surfaces, we have irradiated a copper wafer through a mask that was either (i) a Teflon plate with 2 mm holes or (ii) a chromed quartz mask with 133 μm wide lines (Figure 11C1).

The Teflon mask was used to get an IR image of the spot obtained on the copper wafer with a $40 \times 40\ \mu m^2$ beam size (Figure 11A). The image was recorded at 1600 cm^{-1} (NH_2 deformation vibration) and represents approximately a quarter of the spot. The highest intensity is observed on the upper left corner (center of the spot) in a zone whose dimensions are in agreement with those of the Teflon mask.

With the chromed quartz mask, the resulting lines were imaged by ToF-SIMS. Figures 11B2 and B3 represent the images for, respectively, the sum of the intensities of all positive ions, and the intensity of the

dx.doi.org/10.1021/cm200579b |*Chem. Mater.* 2011, 23, 3449–3459

peak at m/z = 132.99 [$CuCH_2CH(NH_2)CH_2CH^+$]. The latter, which is recorded in the line, is represented in Figure 11B1. Optical images of the quartz mask and the irradiated copper wafer are presented, respectively, in Figures 11C1 and C2. The two images are in good agreement; 166 μm wide lines are visible on the patterned wafer. The same lines were also imaged by optical microscopy (11D1). Profilometry across the line (11D2) permits to measure the thickness and the width of the line: ~40 nm and ~200 μm respectively (in fair agreement with the optical image).

These different images indicate that localized photografting is possible on metals and that the lines observed optically correspond to the organic layer obtained from the photochemical reaction of ACN.

DISCUSSION

The existence of an organic layer on metallic surfaces because of the photochemical grafting of ACN is evidenced by the surface IR spectra, the SEM images, and the Tof-SIMS spectra that are different from those of the background. This layer contains nitrogen as shown by EDS and ToF-SIMS measurements, and this nitrogen is present as amines that are identified through their stretching and deformation bands in IRRAS. IRRAS also shows carbonyl bands and weak nitrile bands, while the latter are very strong in pure acetonitrile. Ellipsometry shows that these layers are in the 10−100 nm range; they are homogeneous as observed by SEM and ToF-SIMS. These layers are strongly bonded to the surface as they resist ultrasonication for 15 min; this strong attachment is due to a chemical bond as evidenced by ToF-SIMS through the peaks containing both a metallic atom and part of the organic layer such as CuC_2H_3N (Figure 10C).

A remarkable difference between photo and electrografting can be mentioned. Under photografting, the thickness of the layer increases linearly with time since the radicals are continuously generated in the solution and bind to the growing layer. Conversely, under electrografting, the layer is self-limiting and reaches a limit after a certain time[74] since the electron must transfer from the electrode to the solution through the layer; as the layer grows, the electron transfer becomes slower and slower and finally stops.

These coatings can be compared with the layers obtained by indirect electrografting of ACN through hydrogen atom

Table 2. Open Circuit Potentials without and under Irradiation (V(Ag/AgCl))

	Cu	Au	Ni	Fe
	−0.34	−0.27	−0.19	−0.12
	−0.37	−0.29	−0.19	−0.11
NH_2 vs C=O[a]	~90:10	~0	~30:70	~50:50

[a] Ratio of IR intensities of the NH_2 deformation and the C=O stretching bands in Figure1B.

Scheme 2

$$Ar^{\bullet} + CH_3CN \longrightarrow ArH + {}^{\bullet}CH_2CN$$

$$Cu + {}^{\bullet}CH_2CN \longrightarrow Cu\text{-}CH_2CN$$

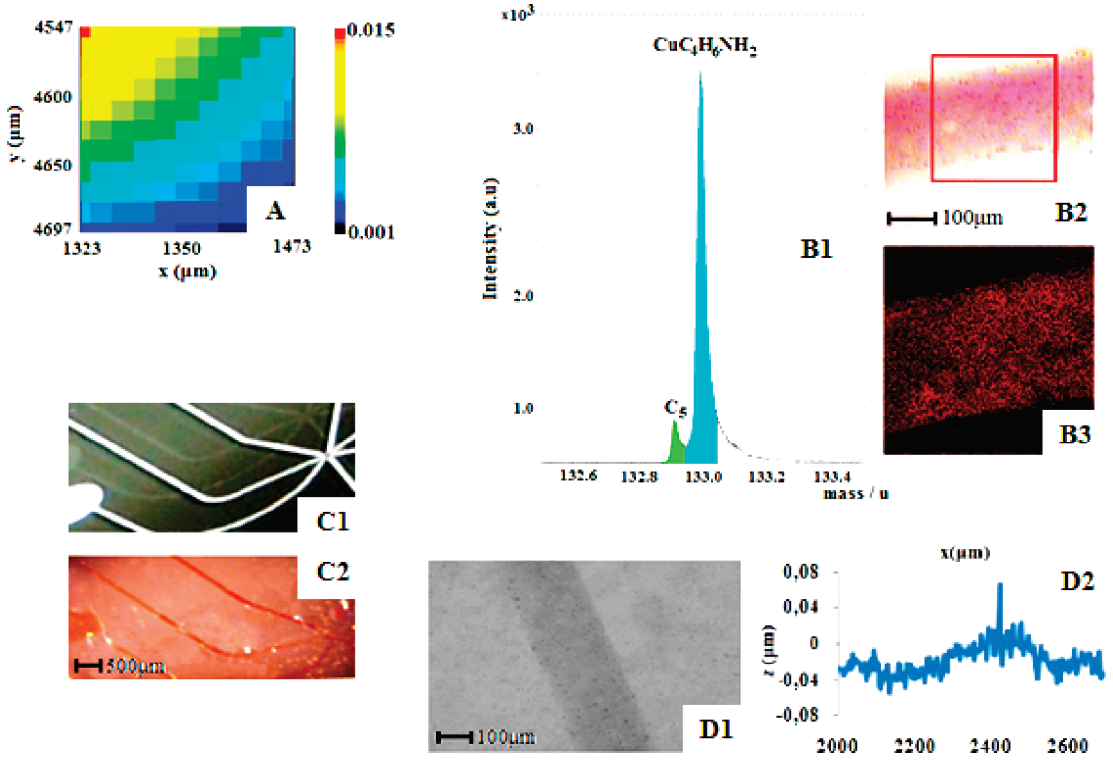

Figure 11. Localized photografting of a copper wafer: (A) IR map of a spot grafted through a Teflon mask with 2 mm holes (40 × 40 μm^2 beam size, recorded at 1600 cm^{-1}). (B−D) Line grafted through a chromed quartz mask with 133 μm wide lines: (B1) Tof-SIMS positive fragments at m/z = 132.99. (B2, B3) images obtained from (B2) the sum of the intensities of all positive ions and (B3) the intensity of the m/z = 132.99 ion (in the red rectangle in B2). (C) optical images of (C1) the mask and (C2) the obtained pattern (note that the scale is nearly the same). (D1) optical image of the grafted line; (D2) the corresponding interferometric profile across the grafted band.

dx.doi.org/10.1021/cm200579b |Chem. Mater. 2011, 23, 3449–3459

Scheme 3

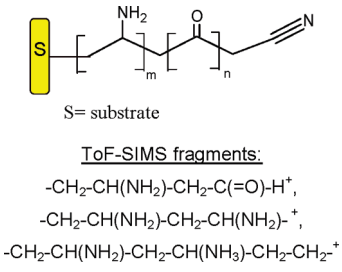

Scheme 4

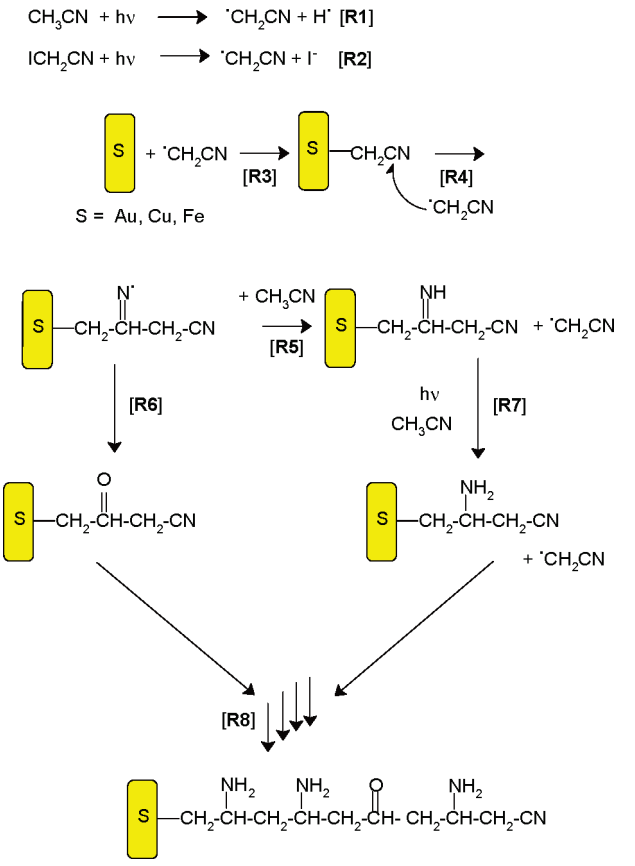

abstraction from ACN by the 2,6-dimethylphenyl radical ($Ar^{\bullet}$)[66] to give the cyanomethyl radical (Scheme 2).

In this case, a structure containing amino and carbonyl groups was assigned to the layer. Here, a similar structure can be assigned to the photografted layer. It is presented in Scheme 3 along with the characteristic ToF-SIMS fragments. The layer obtained on a copper wafer after 10 min irradiation in ACN is 20 nm thick (Figure 6); for comparison, a $-CH_2-CH(NH_2)-$ group is 0.11 nm long.

A mechanism for the formation of the above layers is summarized in Scheme 4. We propose that the same cyanomethyl radical be responsible for the photografting of ACN and ICH_2CN. The photografting of alkyl halides on metals (Cu, Au) under UV irradiation[60] and on diamond surfaces (hydrogenated or not) using X-ray beams[58] or UV irradiation with an Hg arc[59] has been reported, and the alkyl radical was deemed responsible for the reaction with the metal. The electrochemical reduction of I, $BrCH_2CN$ has been described, and the resulting cyanomethyl radical was shown to react with metallic surfaces to give amino layers.[65] The cyanomethyl radical has been previously identified in acetonitrile under irradiation [R1].[68,75] For example, this radical has been characterized by electron spin resonance (ESR) upon irradiation with a mercury lamp.[75a] Therefore, we propose that the cyanomethyl radical is formed by irradiation of either CH_3CN [R1] or ICH_2CN [R2]. It reacts with the surface along reaction [R3].

In the course of indirect electrografting, the growth of the layer was assigned to the reduction of the cyanomethyl radical into the cyanomethyl anion, which further reacts with the nitrile group already grafted to the surface (Thorpe reaction). In this case, the potential of the electrode (−0.90 V(Ag/AgCl) on Au and Cu) or the open circuit potential (−0.44 V(Ag/AgCl) on Cu permitted the reduction of the radical to the anion.[66] Addition of 1% water completely suppressed the grafting reaction by protonation of the anion.

Here, upon addition of 1% water or acetic acid during photograting, there was no change in the IRRAS spectrum of the surface. Moreover, by adding TEMPO, the photografting was completely suppressed, indicating a radical reaction. This clearly shows that (i) no anion and (ii) no electron transfer from the metal to the cyanomethyl radical are involved in the process. The ocp under irradiation (−0.37 V/(Ag/AgCl)) is not very different from the ocp measured during the indirect electrografting in the presence of 0.1 M 2,6-dimethylbenzene diazonium (−0.44 V/(Ag/AgCl)).[66] Therefore, the difference of mechanism between photochemical and electrochemical reactions (radical vs anionic reaction) cannot be explained by different potentials of the metal. It should originate from kinetics differences: the radical reaction would be faster than the anionic reaction under photochemical irradiation because of the increased concentration of the radical. Note that the cyanomethyl radical should be quite stable in ACN as the only reaction it may undergo in solution is a hydrogen atom abstraction from ACN, that regenerates the same radical.

Therefore, we propose that the growth of the layer be due to the attack of the cyanomethyl radical on the nitrile group of the first grafted $-CH_2CN$ group [R4]. The attack of the radical takes place on the carbon atom of the nitrile group. This reaction has already been reported in the literature:[76] (i) the cyanobutyl radical cyclizes to give cyclopentanone through an intermediate iminyl radical,[77] (reaction rate: 4.5×10^2 s^{-1} at 259 K);[78] (ii) iminyl radicals are generated by 5-*exo* cyclization of alkyl, vinyl, and aryl *C*-centered radicals with nitriles;[79] (iii) the fluoroformyl radical reacts with acetonitrile to give an iminyl radical[80] and the ESR spectrum of iminyl radicals has been observed.[81] In Scheme 4, the iminyl radical can be hydrogenated to an imine by hydrogen atom transfer from ACN, regenerating a cyanomethyl radical [R5]; therefore, the reaction is a chain reaction. For comparison, the fast rate constants for the reaction of the 2-methyl-6,6-diphenyl-5-hexeniminyl radical with good hydrogen donors such as thiophenol and chlorothiophenol are: $k = 0.6 \times 10^7$ and 1.4×10^7 M^{-1} s^{-1}, respectively.[82]

The formation of keto groups during the indirect electrografting[66] was assigned to the hydrolysis of the imine during the rinsing of the samples. But in the present photografting reaction, addition of 1% water or acetic acid does not change the $-NH_2/C{=}O$ ratio measured by IRRAS. Therefore, the $-C{=}O$ group does not originate from the hydrolysis of the imine. On gold, in

the absence of dioxygen, the IR intensity of the carbonyl group is smaller but does not completely disappear; on copper this band increases when the copper surface is left in contact with air. This indicates that the sources of oxygen are atmospheric dioxygen *and* the surface oxides [R6]. The differences between the samples prepared with or without sonication indicate that sonication influences the results.[73] For samples prepared under the standard conditions described in the Experimental Section, it is difficult to explain why the −C═O band intensity increases in the order Cu < Fe < Ni < Au; it probably depends on many factors among which are the structure of the oxide, its thickness, and its bond dissociation energy. The high amount of carbonyl groups on gold can be related to the high activity of gold as a catalyst. This catalytic activity has been assigned to the extremely reactive nature of atomic oxygen bound in 3-fold coordination sites on metallic gold. This is the predominant form of O at low concentrations on the surface.[83] The formation of the carbonyl group can originate either from the iminyl radical or from the imine, but imines are stable in the presence of oxygen; therefore the reaction of the iminyl radical both with dioxygen and surface oxides is the most likely route to the carbonyl group [R6].

The photoreduction of imines in the presence of a hydrogen atom donor has been documented;[84,85] it occurs along reaction [R7] that also regenerates the cyanomethyl radical. This leads to amines that have been observed by IRRAS, and chemical derivatization. In the case of indirect electrografting,[66] we had assigned the reduction of the imine into an amine to an electron transfer. We have examined this possibility in the present case by recording the open circuit potential (ocp) for the different metals under irradiation and the ratio of keto to amino groups (Table 2). The order of ocp is Cu, Au, Ni, Fe while that of -NH_2/C═O is Cu, Fe, Ni, Au. This difference of order does not support an electron transfer as the main route to the reduction of the imine.[86]

The chain grows by repeating these reactions of the cyanomethyl radical on the terminal nitrile, giving both amines and keto groups in the chain [R8]. The process is a chain reaction as cyanomethyl radicals are generated through [R5 and R7]. The small nitrile bands observed in IRRAS correspond to the terminal nitrile groups.

Localized grafting through a mask gives a pattern whose size is similar to that of the mask (∼150−200 μm lines). Such pattern size compares well with patterns obtained with SECM. It is a little larger than those obtained with PDMS stamps and 3 orders of magnitude larger than those obtained with polystyrene beads. Clearly, the interest of the method we propose is not in the size that it is possible to reach. But with grafting by irradiation through masks or by SECM, the pattern can be tailored at the micrometer scale, which is the size suited for biological applications. With nanobeads or particles, the pattern is fixed since the patterned zone corresponds to the free electrode surface left between the beads arranged in a hexagonal structure. Smaller patterns would necessitate smaller masks or grids and likely a more powerful UV source.[87]

CONCLUSION

The photochemical grafting of ACN is possible on metals; it gives thin organic layers functionalized with amino and keto groups. This method is quite easy to implement; it only necessitates a UV lamp and a very common solvent. Interestingly, the structure of the layers is similar to that obtained through indirect electrografting or through electrografting of I and $BrCH_2CN$, but the mechanism is different, as indicated by the addition of water that stops the electrografting reaction, but does not change the photografting reaction. Therefore, a mechanism involving only radicals is proposed.

Localized grafting is easily performed by carrying out the photografting reaction through a mask. The size of the pattern, which is similar to that of the mask, compares well with patterns obtained with SECM. The interest of the method is not in the size that it is possible to reach, but in the easiness to implement it in the micrometer range, that is well suited for biological applications. Since amino groups are easily post functionalized, it should be possible to use this localized grafting for the construction of biosensors.

ASSOCIATED CONTENT

Supporting Information. IRRAS spectra for Ni, Fe, Au surfaces photografted with ACN and blank experiments without irradiation, determination of ocp, contact angles. This material is available free of charge via the Internet at http://pubs.acs.org.

AUTHOR INFORMATION

Corresponding Author
*E-mail: jean.pinson@espci.fr.

Present Addresses
[‖]Ecole Normale Supérieure, CNRS-ENS-UPMC 8640, 24 rue Lhomond, 75005 Paris, France.

ACKNOWLEDGMENT

We are grateful to Alchimer society for the Tof-SIMS spectra, to Ms. Sandra Nunige for the SEM spectra, and to Dr Didier Thiébaut and Ms. Ramia Bakain for the ESI-MS spectrum of the solution. The Langlois foundation is acknowledged for financial support to one of us (A.B.).

REFERENCES

(1) Palacin, S.; Bureau, C.; Charlier, J.; Deniau, G.; Mouanda, B.; Viel, P. *ChemPhysChem.* **2004**, *5*, 1468.
(2) (a) Pinson, J.; Podvorica, F. *Chem. Soc. Rev.* **2005**, *34*, 249. (b) Bélanger, D.; Pinson, J. *Chem. Soc. Rev.* **2011**, *40*, 3995.
(3) Brooksby, P. A.; Downard, A. J. *Langmuir* **2005**, *21*, 1672.
(4) Duwez, A.-S.; Cuenot, S.; Jérôme, C.; Gabriel, S.; Jérôme, R.; Rapino, S.; Zerbetto, F. *Nat. Nanotechnol.* **2006**, *1*, 122.
(5) Garrett, D. J.; Lehr, J.; Miskelly, G. M.; Downard, A. J. *J. Am. Chem. Soc.* **2007**, *129*, 15456.
(6) Downard, A. J.; Garrett, D. J.; Tan, E. S. Q. *Langmuir* **2006**, *22*, 10739.
(7) Corgier, B. P.; Bélanger, D. *Langmuir* **2010**, *26*, 5991.
(8) Cougnon, C.; Gohier, F.; Bélanger, D.; Mauzeroll, J. *Angew. Chem., Int. Ed.* **2009**, *48*, 4006.
(9) Matrab, T.; Combellas, C.; Kanoufi, F. *Electrochem. Commun.* **2008**, *10*, 1230.
(10) Hauquier, F.; Matrab, T.; Kanoufi, F.; Combellas, C. *Electrochim. Acta* **2009**, *54*, 5127.
(11) Matrab, T.; Hauquier, F.; Combellas, C.; Kanoufi, F. *ChemPhysChem.* **2010**, *11*, 670.
(12) Combellas, C.; Kanoufi, F.; Nunige, S. *Chem. Mater.* **2007**, *19*, 3830.
(13) Ghorbal, A.; Grisotto, A.; Charlier, F.; Palacin, J.; Goyer, S.; Demaille, C. *ChemPhysChem* **2009**, *10*, 1053.

(14) Charlier, J.; Palacin, S.; Leroy, J.; DelFrari, D.; Zagonel, L.; Barrett, N.; Renault, O.; Bailly, A.; Mariolle, D. *J. Mater. Chem.* **2008**, *18*, 3136.
(15) Charlier, J.; Clolus, E.; Bureau, C.; Palacin, S. *J. Electroanal. Chem.* **2009**, *625*, 97.
(16) Charlier, J.; Baraton, L.; Bureau, C.; Palacin, S. *ChemPhysChem.* **2005**, *6*, 70.
(17) Charlier, J.; Ameur, S.; Bourgoin, J.-P.; Bureau, C.; Palacin, S. *Adv. Funct. Mater.* **2004**, *14*, 125.
(18) Azioune, A.; Storch, M.; Bornens, M.; Thery, M.; Piel, M. *Lab. Chip* **2009**, *9*, 1640.
(19) Allméar, K.; Hult, A.; Rånby, B. *J. Appl. Polym. Sci.* **1988**, *26*, 2099.
(20) Yang, W.; Rånby, B. *J. Appl. Polym. Sci.* **1996**, *62*, 545.
(21) Han, J.; Wang, H. *J. Appl. Polym. Sci.* **2009**, *113*, 2062.
(22) Yong, G.; Zhihua, N.; Huaming, L. *J. Polym. Res.* **2009**, *16*, 709.
(23) Subramanyam, U.; Kennedy, J. P. *J. Polym. Sci., Part A* **2009**, *47*, 5272.
(24) Szunerits, S.; Boukherroub, R. *J. Solid State Electrochem.* **2008**, *12*, 1205.
(25) Kim, C. S.; Mowrey, R. C.; Butler, J. E.; Russell, J. N., Jr. *J. Phys. Chem. B* **1998**, *102*, 9290.
(26) Strother, T.; Knickerbocker, T.; Russell, J. N., Jr.; Butler, J. E.; Smith, L. M.; Hamers, R. J. *Langmuir* **2002**, *18*, 968.
(27) Yang, W.; Baker, S. E.; Butler, J. E.; Lee, C.-s.; Russell, J. N., Jr.; Shang, L.; Sun, B.; Hamers, R. J. *Chem. Mater.* **2005**, *17*, 938.
(28) Lasseter, T. L.; Clare, B. H.; Abbott, N. L.; Hamers, R. J. *J. Am. Chem. Soc.* **2004**, *126*, 10220.
(29) Nichols, B. M.; Butler, J. E.; Russell, J. N., Jr.; Hamers, R. J. *J. Phys. Chem. B* **2005**, *109*, 20938.
(30) Nichols, B. M.; Metz, K. M.; Tse, K.-Y.; Butler, J. E.; Russell, J. N., Jr; Hamers, R. J. *J. Phys. Chem. B* **2006**, *110*, 16535.
(31) Nebel, C. E.; Shin, D.; Takeuchi, D.; Yamamoto, T.; Watanabe, H.; Nakamura, T. *Langmuir* **2006**, *22*, 5645.
(32) Steenackers, M.; Lud, S. Q.; Niedermeier, M.; Bruno, P.; Gruen, D. M.; Feulner, P.; Stutzmann, M.; Garrido, J. A.; Jordan, R. *J. Am. Chem. Soc.* **2007**, *129*, 15655.
(33) Wang, X.; Colavita, P. E.; Metz, K. M.; Butler, J. E.; Hamers, R. J. *Langmuir* **2007**, *23*, 11623.
(34) Nebel, C. E.; Uetsuka, H.; Rezek, B.; Shin, D.; Tokuda, N.; Nakamura, T. *Mater. Res. Soc. Symp. Proc.* **2007**, *956*, 113.
(35) Chong, K. F.; Loh, K. P.; Vedula, S. R. K.; Lim, C. T.; Sternschulte, H.; Steinmüller, D.; Sheu, F.-s.; Zhong, Y. L. *Langmuir* **2007**, *23*, 5615.
(36) Zhong, Y. L.; Chong, K. C.; May, P. W.; Chen, Z.-K.; Loh, K. P. *Langmuir* **2007**, *23*, 5824.
(37) Rezek, B.; Shin, D.; Nebel, C. E. *Langmuir* **2007**, *23*, 7626.
(38) Yang, N.; Uetsuka, H.; Watanabe, H.; Nakamura, T.; Nebel, C. E. *Diamond Relat. Mater.* **2008**, *17*, 1376.
(39) Colavita, P. E.; Sun, B.; Wang, X.; Hamers, R. J. *J. Phys. Chem. C* **2009**, *113*, 1526.
(40) Landis, E. C.; Hamers, R. J. *J. Phys. Chem. C* **2008**, *112*, 16910.
(41) Colavita, P. E.; Sun, B.; Tse, K.-Y.; Hamers, R. J. *J. Vac. Sci. Technol., A* **2008**, *26*, 925.
(42) Colavita, P. E.; Streifer, J. A.; Sun, B.; Wang, X.; Warf, P.; Hamers, R. J. *J. Phys. Chem. C* **2008**, *112*, 5102.
(43) Colavita, P. E.; Sun, B.; Tse, K.-Y.; Hamers, R. J. *J. Am. Chem. Soc.* **2007**, *129*, 13554.
(44) Yu, S. S. C.; Tan, E. S. Q.; Jane, R. T.; Downard, A. J. *Langmuir* **2007**, *23*, 4662.
(45) Lockett, M. R.; Shortreed, M. R.; Smith, L. M. *Langmuir* **2008**, *24*, 9198.
(46) Ellison, M. D.; Buckley, L. K.; Lewis, G. G.; Smith, C. E.; Siedlecka, E. M.; Palchak, C. V.; Malarchik, J. M. *J. Phys. Chem. C* **2009**, *113*, 18536.
(47) Dyer, D. J. *Adv. Polym. Sci.* **2006**, *197*, 47.
(48) Pellegrino, G.; Motta, A.; Cornia, A.; Spitaleri, I.; Fragala, I. L.; Condorelli, G. G. *Polyhedron* **2009**, *28*, 1758.
(49) Moraillon, A.; Gouget-Laemmel, A. C.; Ozanam, F.; Chazalviel, J.-N. *J. Phys. Chem. C* **2008**, *112*, 7158.
(50) Bellec, N.; Faucheux, A.; Hauquier, F.; Lorcy, D.; Fabre, B. *Int. J. Nanotechnol.* **2008**, *5*, 741.
(51) Faucheux, A.; Gouget-Laemmel, A. C.; Allongue, P.; Henry de Villeneuve, C.; Ozanam, F.; Chazalviel, J.-N. *Langmuir* **2007**, *23*, 1326.
(52) Coffinier, Y.; Boukherroub, R.; Wallart, X.; Nys, J.-P.; Durand, J.-O.; Stievenard, D.; Grandidier, B. *Surf. Sci.* **2007**, *601*, 5492.
(53) Ha, T. H.; Park, M.-R.; Park, H. J.; Choi, J.-S.; Kim, G.; Hyun, M. S.; Chung, B. H. *Chem. Commun.* **2007**, *16*, 1611.
(54) Mischki, T. K.; Donkers, R. L.; Eves, B. J.; Lopinski, G. P.; Wayner, D. D. M. *Langmuir* **2006**, *22*, 8359.
(55) Gauthier, N.; Argouarch, G.; Paul, F.; Humphrey, M. G.; Toupet, L.; Ababou-Girard, S.; Sabbah, H.; Hapiot, P.; Fabre, B. *Adv. Mater.* **2008**, *20*, 1952.
(56) Yang, M.; Teeuwen, R. L. M.; Giesbers, M.; Baggerman, J.; Arafat, A.; de Wolf, F. A.; van Hest, J. C. M.; Zuilhof, H. *Langmuir* **2008**, *24*, 7931.
(57) Fabre, B. *Acc. Chem. Res.* **2010**, *43*, 1509.
(58) Smentkowski, V. S.; Yates, J. T., Jr. *Science* **1996**, *271*, 193.
(59) Kim, C. S.; Mowrey, R. C.; Butler, J. E.; Russell, J. N. *J. Phys. Chem. B* **1998**, *102*, 9290.
(60) Chehimi, M. M.; Hallais, G.; Matrab, T.; Pinson, J.; Podvorica, F. I. *J. Phys. Chem. C* **2008**, *112*, 18559.
(61) Harmer, M. A. *Langmuir* **1991**, *7*, 2010.
(62) Yan, M. D.; Cai, S. X.; Wybourne, M. N.; Keana, J. W. F. *J. Am. Chem. Soc.* **1993**, *115*, 814.
(63) Charlier, J.; Clolus, E.; Bureau, C.; Palacin, S. *J. Electroanal. Chem.* **2008**, *622*, 238.
(64) Flavel, B. S.; Gross, A. J.; Garrett, D. J.; Nock, V.; Downard, A. J. *ACS Appl. Mater. Interfaces* **2010**, *2*, 1184.
(65) Combellas, C.; Kanoufi, F.; Osman, Z.; Pinson, J.; Adenier, A.; Hallais, G. *Electrochim. Acta* **2011**, *56*, 1476.
(66) Berisha, A.; Combellas, C.; Kanoufi, F.; Pinson, J.; Ustaze, S.; Podvorica, F. I. *Chem. Mater.* **2010**, *22*, 2962.
(67) Combellas, C.; Jiang, D.; Kanoufi, F.; Pinson, J.; Podvorica, F. I. *Langmuir* **2009**, *25*, 286.
(68) Nakamura, T.; Ohana, T.; Ishihara, M.; Hasegawa, M.; Koga, Y. *Diamond Relat. Mater.* **2008**, *17*, 559.
(69) Socrates, G. *Infrared and Raman Characteristic Group Frequencies*, 3rd ed.; John Wiley & Sons: New York, 2008.
(70) Sheets, R. W.; Blyholder, G. *J. Catal.* **1981**, *67*, 308.
(71) Rozkiewicz, D. I.; Ravoo, B. J.; Reinhoudt, D. N. *Langmuir* **2005**, *21*, 6337.
(72) Acros Organics catalog ; http://www.acros.com, RN 123-42-2
(73) Paulik, M. G.; Brooksby, P. A.; Abell, A. D.; Downard, A. J. *J. Phys. Chem. C* **2007**, *111*, 7808.
(74) Brooksby, P. A.; Downard, A. J. *J. Phys. Chem. B* **2005**, *109*, 8791.
(75) (a) Svejda, P.; Volman, D. H. *J. Phys. Chem.* **1970**, *74*, 1872. (b) Lesiecki, M. L.; Guillory, W. A. *J. Chem. Phys.* **1978**, *69*, 4572. (c) Halpern, J. B.; Tang, X. *Chem. Phys. Lett.* **1985**, *122*, 294. (d) Chuang, C. C.; Wu, W. C.; Lee, M. X.; Lin, J. L. *Phys. Chem. Chem. Phys.* **2000**, *2*, 3877.
(76) de Lijser, H. J. P.; Arnold, D. R. *J. Phys. Chem. A* **1998**, *102*, 5592 and references therein.
(77) (a) Ogibin, Yu. N.; Troyanski, E. I.; Nikishin, G. I. *Izv. Akad. Nauk. SSSR, Ser. Khim.* **1975**, 1461. (b) Ogibin, Yu. N.; Troyanski, E. I.; Nikishin, G. I. *Izv. Akad. Nauk. SSSR, Ser. Khim.* **1977**, 843.
(78) (a) Griller, D.; Schmid, P.; Ingold, K. U. *Can. J. Chem.* **1979**, *57*, 831. (b) Roberts, B. P.; Winter, J. N. *J. Chem. Soc., Perkin Trans. 2* **1979**, 1353.
(79) Russell Bowman, W.; Bridge, C. F.; Brookes, P. *Tetrahedron. Lett.* **2000**, *41*, 8989.
(80) Bucher, G.; Kolano, C.; Schade, O.; Sander, W. *J. Org. Chem.* **2006**, *71*, 2135.
(81) Portela-Cubillo, F.; Alonso-Ruiz, R.; Sampedro, D.; Walton, J. C. *J. Phys. Chem. A* **2009**, *113*, 10005.

(82) Le Tadic-Biadatti, M.-H.; Callier-Dublanchet, A.-C.; Horner, J. H.; Quiclet-Sire, B.; Zard, S. Z.; Newcomb, M. *J. Org. Chem.* **1997**, *62*, 559.
(83) Baker, T. A.; Liua, X.; Friend, C. M. *Phys. Chem. Chem. Phys.* **2011**, *13*, 34.
(84) Coyle, D. J. *Introduction to Organic Photochemistry*, 5th ed; Wiley Interscience: New York, 1998; p 144.
(85) Ortega, M.; Rodriguez, M. A.; Campos, P. J. *Tetrahedron* **2005**, *61*, 11686.
(86) As indicated in the Discussion Section, the open circuit potentials in the indirect electrografting and under irradiation are not very different. Therefore, in the case of Cu there may be some involvement of the electron transfer during the reduction of the imine.
(87) Yee, C. K.; Amweg, M. L.; Parikh, A. N. *J. Am. Chem. Soc.* **2004**, *126*, 13962.